IOPscience iopscience.iop.org

Home Search Collections Journals About Contact us My IOPscience

New perspectives on van der Waals–London interactions of materials. From planar interfaces to carbon nanotubes

This content has been downloaded from IOPscience. Please scroll down to see the full text.

2008 J. Phys.: Conf. Ser. 94 012001

(http://iopscience.iop.org/1742-6596/94/1/012001)

View the table of contents for this issue, or go to the journal homepage for more

Download details:

IP Address: 128.119.50.38
This content was downloaded on 08/10/2013 at 21:04

Please note that terms and conditions apply.

Journal of Physics: Conference Series **94** (2008) 012001 doi:10.1088/1742-6596/94/1/012001

New Perspectives on van der Waals - London Interactions of Materials. From Planar Interfaces to Carbon Nanotubes

R F Rajter[1] and R H French[2]

[1] Department of Materials Science and Engineering, Massachusetts Institute of Technology, 77 Massachusetts Avenue Room 13-5034, Cambridge MA 02139, USA

[2] DuPont Co. Central Research, Exp. Sta. E400-5207, Wilmington DE, 19880-0400

E-mail: `rickrajter@alum.mit.edu and roger.h.french@usa.dupont.com`

Abstract. The drive towards nanoscale assembly necessitates an accurate understanding of all the fundamental forces present in a given system to ensure the greatest chance of success. The van der Waals - London dispersion (vdW-Ld) interaction is the universal, long range, interaction that is present in all materials systems. However, scientists and engineers often either ignore or crudely approximate the vdW-Ld interactions because the calculations often appear impractical due to the 1) lack of the required full spectra optical properties and 2) lack of the proper geometrical formulation to give meaningful results. These two barriers are being actively eliminated by the introduction of robust *ab initio* codes that can calculate anisotropic full spectral optical properties and by proper extensions to the Lifshitz vdW-Ld formulation that take into account anisotropic spectral optical properties as well as novel geometries. These new capabilities are of broad utility, especially in the biological community, because of the difficulty in experimental determination of full spectral optical properties of nanoscale, liquid phase biomolecules. Here we compare 3 levels of complexity of vdW-Ld interactions (optically isotropic planar, optically anisotropic planar, and optically anisotropic solid cylinder) as well as calculate and compare a variety of Hamaker coefficients relevant to these systems. For the latter two, more complex, cases, we use the *ab initio* optical properties of single wall carbon nanotubes (SWCNTs). Our results show the effects of strong optical anisotropy upon the overall vdW-Ld interaction strength as well as the presence of strong dispersion-driven torques in both anisotropic cases, which can play a role in CNT alignment with other CNTs and also preferred CNT alignment directions with optically anisotropic substrates[1, 2].

1. Introduction

van der Waals - London dispersion (vdW-Ld) forces are of considerable importance to scientists and engineers across many disciplines. They are influential in properties ranging from colloidal forces in solution to fracture properties of bulk materials[3]. They are even influential when so-called "stronger" forces, such as electrostatic or polar interactions, are present. For example, it has been proposed that the difference in the static dielectric properties of single wall carbon nanotubes (SWCNTs) is the reason for the successful separation of different chiralities of single stranded DNA - single wall carbon nanotube hybrids in salt elution experiments[4]. These intrinsic dielectric property differences also determine the vdW-Ld interactions and also give rise to differences in vdW-Ld energy as a function of chirality[2]. This may therefore also contribute

© 2008 IOP Publishing Ltd

to the observed ability to separate. Thus the study of vdW-Ld spectra and forces can enrich our understanding of particular phenomena, which is important as scientists are interested in using self-assembly processes to create nanoscale structures and devices.

Despite being important and of interdisciplinary interest, vdW-Ld interactions have a reputation for being intractable or difficult to accurately calculate from a first principles, quantum electrodynamic (QED) approach (i.e. the Lifshitz formulation)[5]. The reasons are two fold: lack of the full spectra optical properties of all the components within the system and the geometry of the system not having an analytically tractable solution. While both of these are still issues today, much progress has been made on both fronts in the past 20 years[3, 6].

First, the formulations have been extended to include everything from an infinite number of layers (stacked in the semi-infinite half-space formulation) to cylinders interacting with each other in salt solutions[7]. Recently, the formulations for solid cylinders were extended even further in order to incorporate optical anisotropy into a solid cylinder - cylinder and cylinder-substrate formulations, which are essential for metallic SWCNTs due to the large degree of optical anisotropy in these materials[2]. A recent book published by Parsegian also contains a large array of vdW-Ld formulations for different geometries[6].

Second, the advent of robust, fast, and reliable *ab initio* codes has allowed for the calculation of full spectral optical properties for materials which are not possible to measure experimentally. Experimental methods like vacuum ultraviolet (VUV) reflectivity for bulk optical properties[8], and transmission valence electron energy loss spectroscopy (VEELS) for interfacial optical properties[8] or reflection VEELS for surfaces[9] are still useful for the characterization of many materials. But for nanoscale materials like SWCNTs, techniques like VEELS still cannot accurately determine the anisotropic spectral optical properties because of the difficulty in isolating, aligning, measuring and then analyzing the measured signals off a single SWCNT . Thus *ab initio* computations of full spectral optical properties eliminate this barrier and fill a gap by offering a way to obtain this data for nanoscale materials with results which are directly comparable.

2. Theory

2.1. vdW-Ld spectra

A brief overview of the link from optical properties[10] to Hamaker coefficients is useful before comparing and contrasting the different vdW-Ld formulations. The way that the particular optical properties are obtained is only relevant if there are particular caveats to consider, such as a particular frequency/energy range where the data tend to not be trustworthy. Beyond that, the various experimental or *ab initio* optical properties are interchangeable, and assuming they have been properly scaled they can be directly transformed into the required vdW-Ld spectra using the appropriate Kramers-Kronig (KK) transformations[10, 6]. For example: A VEELS measurement might give the frequency dependent results in $J_{cv}(eV)$ (interband transition strength form) while the *ab initio* codes give the imaginary part of the dielectric spectrum over real frequencies ($\epsilon''(\omega)$). One can convert between the two via the following:

$$J_{cv}(eV) = \frac{m_o^2}{e^2\hbar^2}\frac{eV^2}{8\pi^2}(\epsilon''(eV) + \imath\epsilon'(eV)) \tag{1}$$

Where m_o is the mass of an electron and e is the charge. The next step is to convert this optical property data into the format used in the Lifshitz formulation (i.e. $\epsilon(\imath\xi)$). This is done by the standard KK transformation.

$$\epsilon(\imath\xi) = 1 + \frac{2}{\pi}\int_0^\infty \frac{\epsilon''(\omega) * \omega}{\omega^2 + \xi^2} d\omega \tag{2}$$

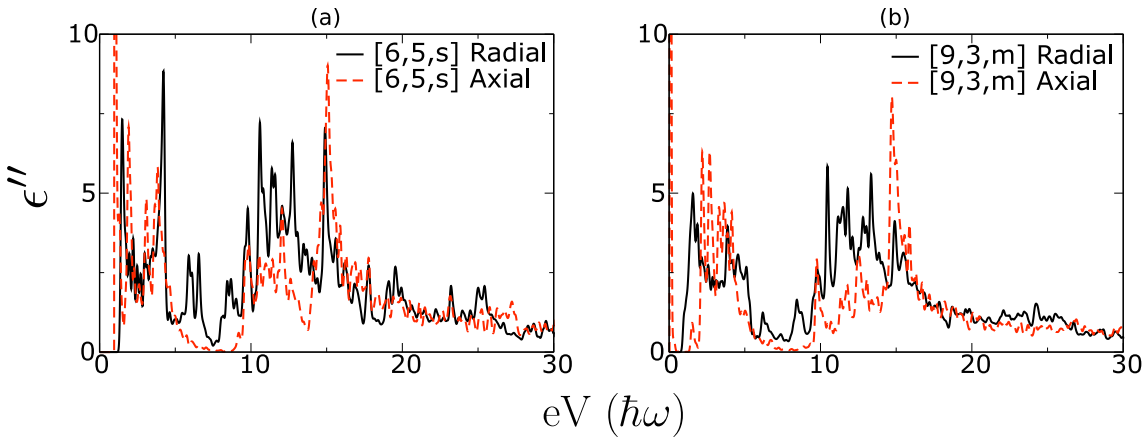

Figure 1. The ϵ'' spectra of the (a) [6,5,s] and (b) [9,3,m] SWCNTs scaled to a solid cylinder geometry. The metallic [9,3,m] SWCNT axial direction spikes to a value of 930 at 0.04 eV.

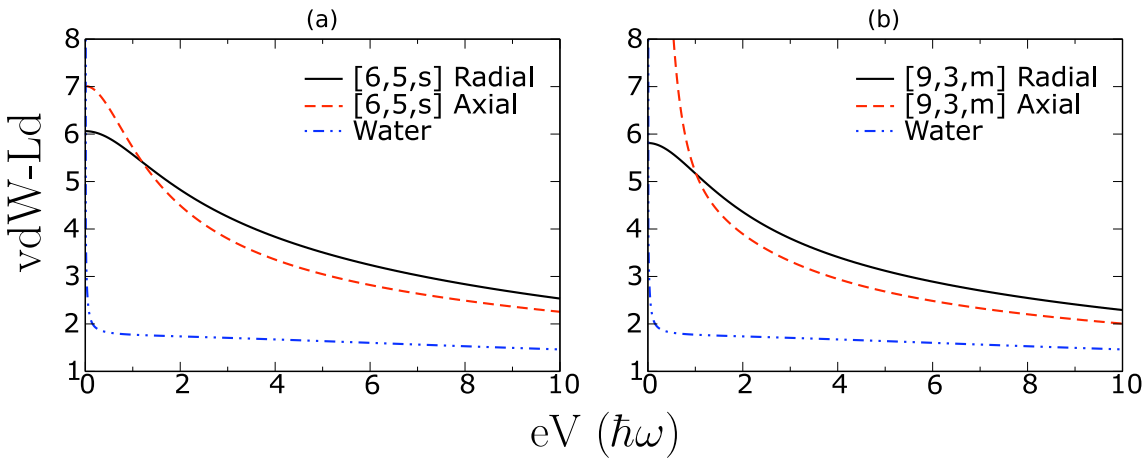

Figure 2. The vdW-Ld spectra of the (a) [6,5,s] and (b) [9,3,m] SWCNTs scaled to a solid cylinder geometry and compared to the index matching water spectra. The [9,3,m] axial direction spikes up to a value of 333 at 0eV.

We typically refer to $\epsilon(\imath\xi)$ as the vdW-Ld spectra in order to differentiate it from the imaginary part of the dielectric spectra term over real frequencies ($\epsilon''(\omega)$). Although these curves typically appear to be simple decaying oscillators, a lot of information can be extracted out of them and small differences in both the magnitude and stacking order can influence the magnitude of the vdW-LD force.

For our SWCNT calculations, we use the ϵ'' properties, from *ab initio* orthogonal linear combination of atomic orbital (OLCAO) computations[11, 12, 13, 14, 15], that have been scaled to the solid cylinder geometry. Figure 1 shows the results for both the [6,5,s] and [9,3,m] SWCNTs in both their axial and radial directions that we obtained previously[2]. We then used Eq 2 to obtain the vdW-Ld spectra as shown in Fig. 1. The metallic [9,3,m] SWCNT has a considerable amount of anisotropy, particularly at energies near 0 eV when the axial direction shoots up to a value of 333.

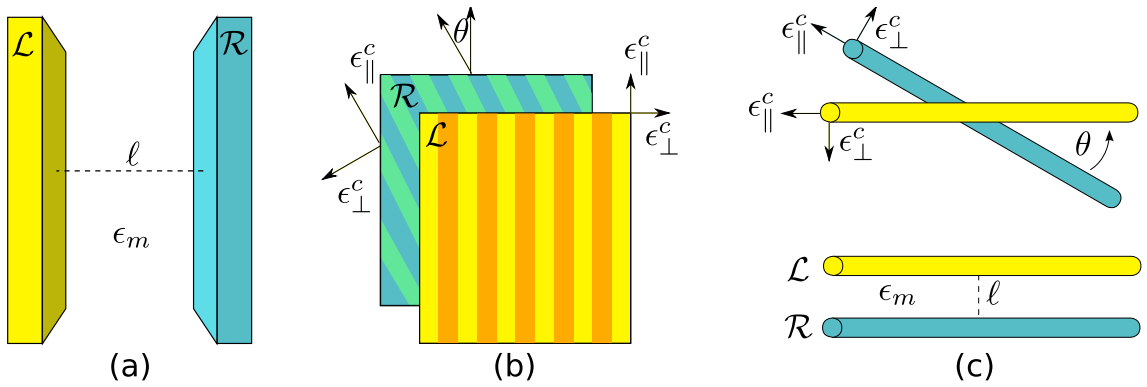

Figure 3. The 3 different systems of comparison. a) Isotropic semi-infinite half spaces b) Anisotropic semi-infinite half spaces c) Anisotropic solid cylinders.

2.2. The General vdW-Ld Framework

Once we have the vdW-Ld spectra of all the relevant materials within a given system, the Lifshitz formulation for that particular geometrical configuration is used to calculate the Hamaker coefficient $\mathcal{A}$. The Hamaker coefficient is then multiplied by the proper geometrical scale factor appropriate to the particular system configuration to determine the interaction energy or force. Thus the general form of the vdW-Ld energy is as follows[1, 6]

$$\mathcal{G} = -\mathcal{A} * \frac{g}{\ell^n} \tag{3}$$

where $\mathcal{G}$ is the free energy, g is a collection of geometry factors (typically consisting of values of π, a coefficient, and perhaps a length dimension of the left or right object), and ℓ^n is the scaling law behavior at a surface to surface separation distance ℓ for a given geometry. Essentially $\mathcal{A}$ is the interaction strength as a function of the material properties of two objects within the given geometrical configuration, whereas g and r are completely independent of $\mathcal{A}$ and determined solely by the system geometry.

The calculation of $\mathcal{A}$ for the non-retarded case [1] over all 3 levels of complexity also has a consistent form across the 3 levels of complexity.

$$\mathcal{A}^{NR} = \frac{3k_bT}{2} * \frac{1}{2\pi}\sum_{n=0}^{\infty}{}' \int_0^{2\pi} \Delta_{Lm}\Delta_{Rm} d\phi \tag{4}$$

where n denotes the discrete Matsubara frequencies ($\xi_n = \frac{2\pi k_b T}{\hbar} n$) ranging from 0 to ∞, the values Δ_{Lm} and Δ_{Rm} are the spectra mismatch functions comparing the vdW-Ld spectra properties of the particular material L or R with the neighboring medium m. The prime on the summation denotes that the first frequency $n = 0$ is multiplied by 0.5.

It is with this general form that we can begin analyzing and compare all 3 systems.

2.3. Isotropic Planar System

The isotropic plane - plane system (see Fig. 3 a) is the most commonly used of all the Lifshitz formulations because it is by far the easiest to calculate and it is the most relevant for the

[1] In the non-retarded case, we neglect the finite speed of light traveling back and forth between the interacting sides.

interactions of large bulk materials. Its energy per unit area is

$$\mathcal{G} = \frac{\mathcal{A}^{NR}}{12\pi\ell^2} \tag{5}$$

Because the left and right half-spaces are both isotropic, there is no angular dependance of the vdW-Ld interaction for rotations about the interface normal of either half space. Therefore the integration around angle $d\phi$ leads to constant value of 2π which cancels out the $\frac{1}{2\pi}$ coefficient in the general form to leave us with

$$\mathcal{A} = \frac{3k_bT}{2}\sum_{n=0}^{\infty}{}' \Delta_{Lm} * \Delta_{Rm} \tag{6}$$

The Δ_{Lm} and Δ_{Rm} terms are as follows

$$\Delta_{Lm}(\imath\xi_n) = \frac{\epsilon_L(\imath\xi_n) - \epsilon_m(\imath\xi_n)}{\epsilon_L(\imath\xi_n) + \epsilon_m(\imath\xi_n)} \quad \Delta_{Rm}(\imath\xi_n) = \frac{\epsilon_R(\imath\xi_n) - \epsilon_m(\imath\xi_n)}{\epsilon_R(\imath\xi_n) + \epsilon_m(\imath\xi_n)} \tag{7}$$

We normally drop the explicit $(\imath\xi_n)$ notation for clarity as it is assumed that all vdW-Ld spectra are frequency dependent and only calculated at each Matsubara frequency (ξ_n) (where each n represents a change of 0.16 eV for the case of 300 K).

2.4. Anisotropic Planar System

As we move to the next level of complexity, we eliminate the assumption of isotropic spectral optical properties and allow the substrates to have optically uniaxial properties with 2 vdW-Ld spectra for directions parallel $\epsilon_{\|}$ and perpendicular to the optical axis of the material. In our particular derivation, we confine the formulation to only allow rotations of the optical axis within direction of the planar interface (see Fig. 3 b). This restriction leads to the appropriate geometrical formulation appropriate for the case of a SWCNT interacting with a packed array of aligned SWCNTs[2]. In principle, one can arrange the 2 substrates so $\epsilon_{\|}$ has an arbitrary relationship to the interface and leads to a component normal to the planar interface if one so chooses.

Because of the angular dependance that arises, the overall vdW-Ld energy now has 2 components $\mathcal{A}^{(0)}$ and $\mathcal{A}^{(2)}$.

$$\mathcal{G} = -\frac{\mathcal{A}^{(0)} + \mathcal{A}^{(2)}\cos^2\theta}{12\pi\ell^2} \tag{8}$$

Here $\mathcal{A}^{(0)}$ represents the Hamaker coefficient when the left and right half-space have their optical axes ($\epsilon_{\|}$) 90 degrees out of phase. As θ, the angle between the optical axes of the left and right half spaces, goes to 0, we get an additional energy contribution from $\mathcal{A}^{(2)}$. $\mathcal{A}^{(0)}$ can be calculated by itself, but the angular contribution is calculated by taking the aligned case $(\mathcal{A}^{(0)} + \mathcal{A}^{(2)})$ and subtracting off $\mathcal{A}^{(0)}$. The form for both endpoints is created by adding the angular dependance to the generalized form to get:

$$\mathcal{A}^{(0)} = \frac{3k_bT}{2} * \frac{1}{2\pi}\sum_{n=0}^{\infty}{}' \int_0^{2\pi} \Delta_{Lm}(\phi)\Delta_{Rm}(\phi - 90)d\phi \tag{9}$$

$$\mathcal{A}^{(0)} + \mathcal{A}^{(2)} = \frac{3k_bT}{2} * \frac{1}{2\pi}\sum_{n=0}^{\infty}{}' \int_0^{2\pi} \Delta_{Lm}(\phi)\Delta_{Rm}(\phi)d\phi \tag{10}$$

Now we just need to consider the detailed forms of Δ_{Lm} and Δ_{Rm} and how these are calculated for this scenario. They are as follows:

$$\Delta_{\mathcal{L}m}(\phi) = \left(\frac{\epsilon_\perp(\mathcal{L})\sqrt{1+\gamma(\mathcal{L})\cos^2\phi} - \epsilon_m}{\epsilon_\perp(\mathcal{L})\sqrt{1+\gamma(\mathcal{L})\cos^2\phi} + \epsilon_m}\right) \tag{11}$$

$$\Delta_{\mathcal{R}m}(\phi) = \left(\frac{\epsilon_\perp(\mathcal{R})\sqrt{1+\gamma(\mathcal{R})\cos^2\phi} - \epsilon_m}{\epsilon_\perp(\mathcal{R})\sqrt{1+\gamma(\mathcal{R})\cos^2\phi} + \epsilon_m}\right) \tag{12}$$

$$\Delta_{\mathcal{R}m}(\phi-90) = \left(\frac{\epsilon_\perp(\mathcal{R})\sqrt{1+\gamma(\mathcal{R})\sin^2\phi} - \epsilon_m}{\epsilon_\perp(\mathcal{R})\sqrt{1+\gamma(\mathcal{R})\sin^2\phi} + \epsilon_m}\right) \tag{13}$$

where γ, a measure of the optical anisotropy for the left or right half-spaces in the near limit, is of the form

$$\gamma = \frac{\epsilon_\parallel - \epsilon_\perp}{\epsilon_\perp} \tag{14}$$

If the parallel and perpendicular epsilons are equivalent, then $\gamma = 0$ and the above Δ terms reduce to Eq.7.

2.5. Anisotropic Solid Cylinders

Things get more interesting and complex as we now change the geometry of the system from two interacting substrates to interacting cylinders. First the energy is now on a per unit length basis for two parallel aligned SWCNTs

$$G(\ell,\theta=0) = -\frac{3(\pi a^2)^2(\mathcal{A}^{(0)}+\mathcal{A}^{(2)})}{8\pi\ell^5} \tag{15}$$

or as total energy when the two SWCNTs are misaligned

$$G(\ell,\theta) = -\frac{(\pi a^2)^2(\mathcal{A}^{(0)}+\mathcal{A}^{(2)}\cos^2\theta)}{2\pi\ell^4\sin\theta} \tag{16}$$

Next, we need a determination of $\mathcal{A}$. If we move towards solid cylinders far away from a substrate, we can use the *Pitaevskii* method[6] for dilute rods in solution and deduce the relevant Δ_{Rm} and Δ_{Lm} terms. The derivation is tedious, but straightforward[2, 7]. The result is

$$\Delta_{\mathcal{L}m}(\phi) = -\left(\Delta_\perp(\mathcal{L}) + \tfrac{1}{4}(\Delta_\parallel(\mathcal{L}) - 2\Delta_\perp(\mathcal{L}))\cos^2\phi\right) \tag{17}$$

$$\Delta_{\mathcal{R}m}(\phi) = -\left(\Delta_\perp(\mathcal{R}) + \tfrac{1}{4}(\Delta_\parallel(\mathcal{R}) - 2\Delta_\perp(\mathcal{R}))\cos^2\phi\right) \tag{18}$$

$$\Delta_{\mathcal{R}m}(\phi-90) = -\left(\Delta_\perp(\mathcal{R}) + \tfrac{1}{4}(\Delta_\parallel(\mathcal{R}) - 2\Delta_\perp(\mathcal{R}))\sin^2\phi\right) \tag{19}$$

where

$$\Delta_\parallel = \frac{\epsilon_\parallel - \epsilon_m}{\epsilon_m} \qquad \Delta_\perp = \frac{\epsilon_\perp - \epsilon_m}{\epsilon_\perp + \epsilon_m} \tag{20}$$

Although these Δ terms are different in appearance from the previous two formulations, the calculations are just as straightforward from a computational standpoint. However, it is within these newly introduced anisotropic terms $\Delta_\parallel$, $\Delta_\perp$, and γ that new and interesting phenomena arises, which will be discussed in more detail later.

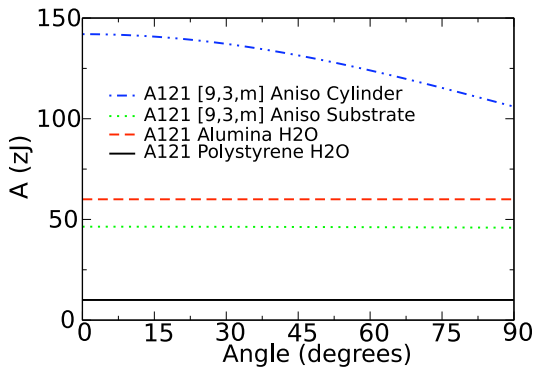

Figure 4. Comparing the Hamaker coefficients across all 3 systems. The polystyrene and alumina coefficients were both calculated using the isotropic planar formulation while the [9,3,m] spectra was used in both the anisotropic planar and anisotropic cylinder formulations.

3. Results

For the optically isotropic-planar case we use full spectral optical properties of alumina[16] and polystyrene[17] across water. The water spectra is developed from the index of refraction oscillator model detailed in Parsegian[6]. There have been many optical property models developed for water[18, 19], but we believe this to be the most appropriate for vdW-Ld interactions in colloidal systems since it properly captures the zero frequency term as well as reproducing the index of refraction in the visible region (which is essential due to the large number of UV and VUV terms in the Lifshitz summation). The calculations were both done using Gecko Hamaker[20].

For both the optically anisotropic planar and optically anisotropic solid cylinder systems, we used the full spectral optical properties for the [9,3,m] and [6,5,s] SWCNTs scaled to a solid plane and a solid cylinder, respectively, and the same index matching water spectra used in the isotropic case. The calculations were done in *Mathematica* that is available at the Gecko Hamaker website[20].

Figure 4 shows the resulting Hamaker coefficients for all 3 systems. The [9,3,m] solid cylinder SWCNTs have by far the strongest Hamaker coefficient and exhibit the largest degree of anisotropy, increasing in magnitude from 106 zJ to 142 zJ (approximately 34%). The [9,3,m] solid substrates have a smaller overall Hamaker coefficient (46 zJ) and gain just over 0.5 zJ when switching from the perpendicular to parallel (co-linear) geometry. Alumina and polystyrene are isotropic and have values of 60 zJ and 10 zJ respectively.

Fig. 5 looks more closely at the difference in angular dependance on the Hamaker coefficient between the [6,5,s] and the [9,3,m] solid cylinders in the far limit (defined as separations greater than 2 times the SWCNT cylinder diameter). The [6,5,s] is a weaker interaction at all angles, but does manage to gain an additional 2 zJ in its Hamaker coefficient upon aligning.

4. Discussion

The appealing aspect of comparing these 3 forms of the vdW-Ld interactions simultaneously is the ease by which one can travel between them. One can start complex at the level of anisotropic solid cylinders and then use their isotropic spectra and eliminate the torques from

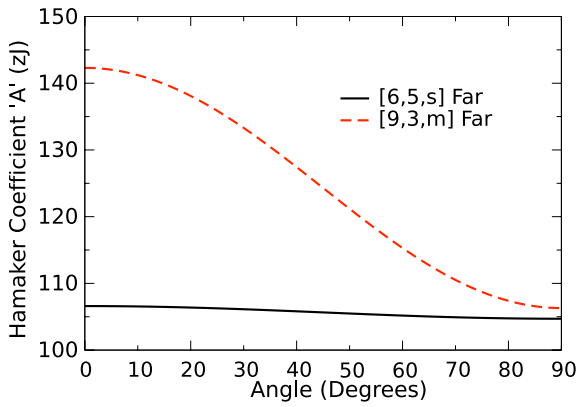

Figure 5. The angular dependence upon the far limit aniso cylinder - aniso cylinder interaction for the [6,5,s] and [9,3,m] SWCNTs

appearing ($\mathcal{A}^{(2)} = 0$). Or one can start off with isotropic planes and work up by introducing optical and geometrical/morphological anisotropy. Figure 6 shows the complete break down of all three scenarios, starting with the geometrical arrangement and working down to the basic components.

4.1. Comparing and Contrasting the Equations

As mentioned above, all 3 forms have the same structure at the top level. That is, there is some Hamaker coefficient being multiplied by some geometric scale factors and distance scaling law behavior. The Hamaker coefficient is then determined by summing up the interactions of spectral mismatch functions (the Δ_{Lm}'s). It is these spectral mismatch functions, Δ_{Lm} where all the variation begins (see Figure 6).

The biggest change that occurs when moving to the more complex systems is the introduction of anisotropic terms into the spectral mismatch functions. In the anisotropic planar system, we get γ while the far limit, anisotropic solid cylinder system introduces $\Delta_\perp$ and $\Delta_\parallel$. Of the three, $\Delta_\parallel$ is by far the most influential for the magnitude of the overall Hamaker coefficient and torque. The reason for this is due to the change in the fractional form from $\frac{a-b}{a+b}$ (e.g. $\Delta_\perp$ and equations7) to an asymmetric form $\frac{a-b}{b}$. When any Δ is of the form $\frac{a-b}{a+b}$, its contribution can never exceed 1 within the summation of the Lifshitz formulation. Thus there is a finite maximum ceiling limit as to how large the Hamaker coefficient can be. However, for large differences in spectra properties, terms like γ and $\Delta_\parallel$ can far exceed 1 and add a large contribution to the overall coefficient.

For example: For the [9,3,m] SWCNT immersed in water at the $n = 1$ Matsubara frequency, the values of γ, $\Delta_\perp$, and $\Delta_\parallel$ are 5.8, 18.6, and 0.5 respectively. This is why the far limit solid cylinder Hamaker coefficients are much larger than the anisotropic plane-plane formulation. Now γ itself is also a fairly large value at this particular frequency, but we must also remember that γ is found under a square root sign wherever it appears, so its effect is dampened (but still noticeable) when compared to the far limit anisotropic cylinder case.

The large value of $\Delta_\parallel$ is also the origin of the large degree of anisotropy. If we observe equation 19 we can see that for the $\mathcal{A}^{(0)} + \mathcal{A}^{(2)}$ case, the left and right Δ terms will integrate together in phase and the large $\Delta_\parallel$ terms will multiply together. When 90 degrees out of phase, $\Delta_\parallel$ will be multiplied by a much smaller $\Delta_\perp$. To put some numbers behind this, using the values at Matsubara frequency $n = 1$ as given above, equation 19 yields $\Delta_{\mathcal{R}m}(\phi = 0) = 4.9$ while $\Delta_{\mathcal{R}m}(\phi = 90) = 0.5$. Over the entire integral of all 2π in plane directions, $\Delta_{\mathcal{L}m}(\phi) * \Delta_{\mathcal{R}m}(\phi) =$

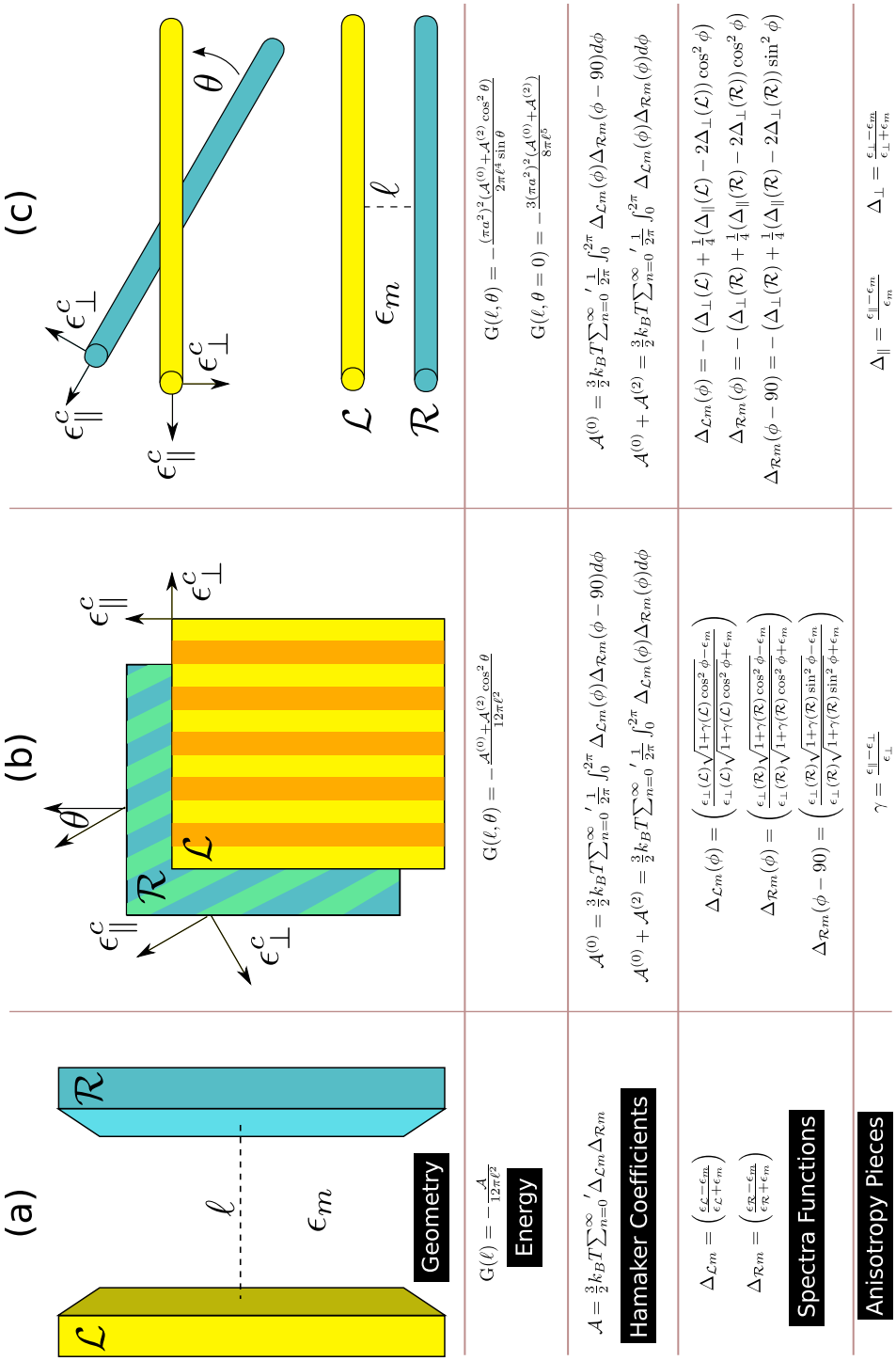

Figure 6. The overall layout comparing the different layers of abstraction among all the geometries. The calculation starts with a particular geometry, which then defines the energy scaling law behavior $\mathcal{G}$ and the particular form of the Hamaker coefficient calculation $\mathcal{A}$. Each particular formulation's Hamaker coefficient is comprised of specific spectra mismatch functions. The anisotropic systems have an additional level of abstraction beyond the mismatch functions that consists of the anisotropic terms γ, $\Delta_{\parallel}$, and $\Delta_{\perp}$.

56.5 while the 90 degree offset version $\Delta_{\mathcal{L}m}(\phi) * \Delta_{\mathcal{R}m}(\phi - 90) = 18.8$. While the other Matsubara frequencies do not contribute nearly as strong as the n=1 term, they all influence $\mathcal{A}^{(2)}$ in making it as large as it is for the [9,3,m]. For the [6,5,s], the largest value of $\Delta_{\|}$ is around 3.0 and thus this SWCNT definitely has some anisotropy, but not nearly as much as the [9,3,m].

4.2. Caveats, Assumptions, and Moving Forward

Although these new formulations represent a substantial step forward in our ability to calculate Hamaker coefficients for systems as complicated as SWCNTs, there are a few shortcomings that are inherent in the present formulation and results. The biggest and most important is the current loss of the ability to include retardation (i.e. the effects of distance and the finite speed of light). This was a necessity in our first steps into systems of this complexity because of the difficulty in getting analytically tractable solutions that are generic and understandable enough for general utility without having to go forward with only brute force numerical calculations. However, now that this current position is established, we can move forward and see (using particular limits and limiting cases), when we can include things like retardation or the very important role of coatings on cylinders to give an even better understanding of the role and behavior of the vdW-Ld interactions at these length scales.

4.3. Utility of Ab Initio Optical Properties and Cylinder Formulations for Biological Systems

The ability to get optical properties from *ab initio* calculations, coupled with advances in the ability to calculate Hamaker coefficients for more complex configurations represents a substantial leap forward in our ability to calculate vdW-Ld properties. For example, say we want to know the vdW-Ld interaction between the triple helix layers of collagen. We have already calculated the anisotropic optical properties of collagen and found them to be fairly isotropic. Since the triple helix is, to a first approximation, equivalent to abutting solid cylinders, we could in fact use a near limit solid cylinder formulation of $\mathcal{A}$ and the scale factor to get a reasonable estimate of the total vdW-Ld energy for comparison to the thermal energy in an aqueous solution. This can be done for any number of different polymers, proteins, ssDNA, or any other particle useful in the creation of nano-scale devices. Knowing what the vdW-Ld interaction energies are can aid in the selection of one particular material type, configuration or geometry over others based on the desired interaction strength.

5. Conclusions

Here we have shown how new formulations and the ability to obtain full spectra optical properties from *ab initio* codes allows us to further extend the ability to calculate vdW-Ld interactions for complex systems. We also illustrated that these new formulations are merely adjustments at the lower levels of abstraction of previous formulae, and thus are no more difficult to use and implement than the original Lifshitz plane-plane formulation. However, these new formulations are very important to utilize when the system requires it because they effect more than just the torque, but can effect the overall Hamaker coefficient magnitude as seen by the [9,3,m].

6. Acknowledgements

We would like to acknowledge Wai Yim Ching, Adrian Parsegian, Rudi Podgornik, Yet-Ming Chiang, and W. Craig Carter for all helping to make this work possible.

References

[1] Rajter R F, French R H, Ching W Y, Carter W C and Chiang Y M 2007 *J. Appl. Phys.* **101** 054303
[2] Rajter R F, Podgornik R, Parsegian V A, French R H and Ching W Y 2007 *Phys. Rev. B.* Accepted
[3] French R H 2000, *J. Am. Ceram* **83** 2117
[4] Lustig S R, Jagota A, Khripin C and Zheng M 2005. *J. Phys. Chem.* **109** 2559

[5] Lifshitz E M 1956. *Sov. Phys. JETP* **2** 73
[6] Parsegian V A 2005. *Van der Waals Forces*, Cambridge University Press, Cambridge
[7] Podgornik R and Parsegian V A 1998. *Phys. Rev. Lett.* **80**, 1560
[8] Tan G L, Lemon M F, French R F and Jones D J 2005. *Phys. Rev. B* **72** 205117
[9] Tan G L, DeNoyer L K, French R H, Guittet M J and Gautier-Soyer M 2004. *J. of Electron Spectroscopy and Related Phenomena* **142** 97
[10] Wooten F 1972. *Optical Properties of Solids*, Academic Press, New York
[11] Ching W Y 1990. *J. of Amer. Ceram. Soc.* **71** 3135
[12] French R H, Glass S J, Ohuchi F S, Xu Y N and Ching W Y 1994. *Phys. Rev. B* **49** 5133
[13] Ching W Y, Xu Y N and French R H 1996. *Phys. Rev. B* **54** 13546
[14] Xu Y N, Ching W Y and French R H 1993. *Phys. Rev. B* **48** 17695
[15] Xu Y N and Ching W Y 1995. *Phys. Rev. B* **51** 17379
[16] Palik E D (Editor). *Handbook of Optical Constants of Solids* Vol. I, 1985; Vol II, 1991; Vol. III, 1998. Academic Press, New York
[17] French R H, Winey K I, Yang M K and Qiu W 2007. *Aust. J. Chem.* **60** 251
[18] Ackler H D, French R H and Chiang Y M 1996. *J. Colloid Interface Sci.* **179** 460
[19] Dagastine R R, Prieve D C and White L R 2000. *J. Colloid Interface Sci.* **231**, 351
[20] see http://sourceforge.net/projects/geckoproj